Received: 22 February 2024 | Revised: 17 April 2024 | Accepted: 30 May 2024 | Published online: 6 June 2024

RESEARCH ARTICLE

Artificial Intelligence and Applications
2024, Vol. 2(4) 315–329
DOI: 10.47852/bonviewAIA42022662

BON VIEW PUBLISHING

# A Supervised Machine Learning Monitoring System for Vehicle-Railway Bridge Collision

**Khaled Hallak[1,*] and Adel Abdallah[1]**

[1]*University of Lorraine, France*

**Abstract:** Vehicle collision on bridges is an important issue for the transportation infrastructure management. This study explores the significance of bridge monitoring and the benefits of employing machine learning (ML) techniques to detect and classify vehicle-deck collisions on railway bridges. The ultimate goal is to transition from traditional bridge monitoring methods to a real-time monitoring system based on a ML approach, aiming to improve efficiency and accuracy in detecting bridge issues. Multiple supervised ML algorithms are evaluated to identify the most accurate model for collision detection and signal categorization. The selected ML model employs a distributed approach, enhancing its adaptability and integration into a comprehensive monitoring system for diverse bridge structures. The dataset comprises frequency, velocity, and displacement measurements collected over a one-year monitoring period from three distinct railway bridges. Additionally, a controlled experiment was conducted to identify signal patterns associated with collisions of different energy levels. The collected data underwent rigorous processing, including data cleaning, synchronization, pattern identification, and statistical analysis, to extract relevant features. The proposed model achieved an accuracy of 100% in detecting vehicle-deck collisions on railway bridges and demonstrated high accuracy in classifying other types of signals. The model provides bridge managers with a valuable digital decision support tool that aids in evaluating bridge conditions, minimizing maintenance costs, and ensuring train user safety. Furthermore, the developed approach aids in reducing disk storage and saving energy in embedded systems, enhancing its practicality and sustainability in real-world applications.

**Keywords:** supervised machine learning, distributed machine learning, anomaly detection, structural health monitoring, vehicle-bridge collisions, railway bridges, classification model

## 1. Introduction

Railway bridges are exposed to various factors that can lead to structural degradation and potential failure, including environmental conditions, constant wear and tear, and unforeseen circumstances. If not identified and addressed promptly, these issues can result in malfunctioning, reduced structural integrity, and even catastrophic failures, potentially causing significant loss of life and property damage.

Railway bridges are particularly vulnerable to collisions with road vehicles crossing beneath the bridge. These incidents can occur when vehicles directly impact the bridge structure or carry oversized cargo exceeding clearance height restrictions. Public works machinery also poses a threat, as mobile elements like buckets, mechanical shovels, and crane jibs may fail to retract to a low position when passing under the bridge. These incidents represented up to 50% of incidents recorded on bridges managed by the French railway network administrator (SNCF-R) [1], over the past decade. Moreover, more than 35% of the 300,000 railway bridges across Europe are over 100 years old, and their reliability directly impacts the reliability of the railway network [2]. Numerous collisions may go undetected, yet certain incidents can have severe consequences, necessitating a temporary stoppage of railway traffic for prompt maintenance to ensure user safety.

Recent catastrophic railway bridge failures underscore the critical need for robust monitoring and maintenance practices. These failures include the Kadalundi train disaster [3] of June 22, 2001, in India, caused by fatigue cracks in the steel superstructure, resulting in the loss of 59 lives and injuries to up to 300 people; the Valigonda rail disaster of 2005 [4], which claimed the lives of 114 people and injured over 200; and the Big Bayou Canot Bridge accident in 1993 [5], which resulted in the tragic loss of 47 lives and 103 more were injured. These examples highlight the imperative for vigilance and preventive measures to ensure the safety and integrity of railway bridges.

Traditional bridge monitoring methods typically rely on periodic visual inspections [6], which can be time-consuming, expensive, and may miss subtle signs of damage (e.g., limited accessibility and difficulty in identifying early signs of damage). In recent years, the use of sensors attached to bridges has emerged as a promising approach for continuous structural health monitoring (SHM) of bridges [7, 8]. Machine learning (ML) techniques, particularly anomaly detection, present a compelling solution for addressing these challenges. Unlike traditional methods, ML algorithms can analyze complex patterns and

*Corresponding author: Khaled Hallak, University of Lorraine, France. Email: khaled.hallakhammoud@cea.fr

relationships within large datasets [9], enabling the detection of subtle anomalies that may be overlooked by human inspection or basic traditional approaches. Moreover, ML models can adapt and learn from new data, improving performance over time and enabling the detection of evolving or previously unseen anomalies. While traditional methods may provide some level of success, they often lack the robustness and predictive capability of ML approaches. The integration of ML with bridge monitoring offers significant advantages, including early detection of structural problems, reduction of maintenance costs, and improvement of safety measures. However, several factors make the anomaly detection on railway bridges a challenging approach, such as the uncertainty/variability of sensor measurements, the varying complexity of bridge structures, and the availability of labeled data for training/validation of models.

Several studies have investigated the application of ML techniques for SHM. For instance, Ghiasi et al. [10] introduced a KNN-based approach (K-Nearest Neighbors) for detecting corrosion in steel railway bridges, achieving high accuracy in classifying cross-section losses due to corrosion damages. They utilized data from continuous wavelet transform scalograms and Bayesian Modal Identification method. Another study by Ghiasi et al. [11] employed a vibration-based deep learning approach using convolutional neural networks for corrosion-induced cross-section loss classification, showcasing close to 100% accuracy. Moreover, Wang et al. [12] presented a method for anomaly detection in high-speed railway track monitoring data, utilizing robust sparse Bayesian learning and broad learning techniques. This approach demonstrated advantages over traditional methods in noise robustness, pattern identification flexibility, and real-time monitoring efficiency, effectively detecting various damage types. Another study by Lee et al. [13] introduced a Bayesian method for monitoring abnormal structural responses induced by high-speed trains, offering insights into dynamic amplifications through probabilistic monitoring of time-history deflections. Chalouhi et al. [14] proposed a model using artificial neural networks (ANN) and Gaussian Processes for damage detection and localization in railway bridges, showing good agreement with previous studies and effectively detecting anomalous responses during train passages. Abdu et al. [15] assessed railway bridge pier settlement using ML algorithms, achieving high accuracy in predicting settlement with ML models trained on train acceleration response data. Akintunde et al. [16] introduced a data-driven method for estimating strain at unmeasured locations on operational railway bridges, demonstrating accurate strain estimations with significantly lower error compared to traditional model-based methods through k-means clustering and self-organizing maps.

Inspired by the successes of these prior studies, the present research explores the importance of bridge monitoring and explores the advantages of ML techniques in detecting and characterizing vehicle-deck collisions on railway bridges. While many studies have investigated the use of ML for improving the monitoring system of railway bridges, most have focused on the effects of trains passing over the railway or cars passing above a bridge. This study, in contrast, focuses on the detection and analysis of shocks caused by high vehicles passing beneath the railway bridge. This distinction is important because vehicle-deck collisions can have a significant impact on the structural integrity of bridges, making them a critical area of concern for bridge managers. The ultimate goal is to develop a comprehensive monitoring system that integrates the classification model directly into the sensor network and operates as a real-time streaming system. The unique aspect of this system is its ability to be applied to bridges of various structures and dimensions. In this study, various supervised ML algorithms are compared to identify the optimal model with the highest accuracy for detecting vehicle-deck collisions on railway bridges. The performance of these models will be evaluated based on various metrics, including accuracy, precision, recall, and *F*1-score. The models developed in this study employ several features as input, such as frequency, velocity, and displacement measurements. Unlike previous studies that primarily relied on raw data [13, 14], the proposed approach uses only signal features (e.g., maximal Velocity and dominant frequency). This approach minimizes disk storage requirements while preserving critical information for analysis, marking a significant departure from conventional methods. Furthermore, the used sensor leverages solar energy for power, offering a sustainable and environmentally friendly solution compared to energy-intensive sensors used in prior studies. A large amount of data collected over a one-year monitoring period from three different railway bridges is used in this study. Additionally, a controlled experiment was performed on a bridge to recognize the signals' patterns associated with collisions of varying energy, to ensure accurate classification and labeling of the monitoring data to be used. Prior to applying statistical methods to analyze potentially patterns and extract relevant features, the obtained data is thoroughly cleaned and synchronized. The main objective of the study is to classify different types of signals generated by the sensors installed on the bridges and identify the major impact shocks that may put the bridge in danger and require immediate maintenance. Furthermore, this project aims to minimize future maintenance costs by enabling proactive maintenance and timely interventions based on the detected signals. The obtained results can provide a digital decision support tool for bridge managers, enabling them to effectively address the structural condition of bridges.

This paper is divided into four sections. In the first section, the context of the study is presented, then the instrumentation design and implementation are detailed. The second section will cover data preprocessing, including cleaning, synchronization, partitioning, as well as signal pattern identification and data labeling. The third section focuses on the development of multiple ML models and compares the results to identify the most suitable one. The fourth section analyzes and discusses the obtained results to finally conclude with future research perspectives.

## 2. Materials and Methods

### 2.1. Instrumentation

The instruments used for monitoring the bridges are accelerometer, displacement sensors, and photographic trap.

#### *2.1.1. Accelerometer*

A Micro-Electro-Mechanical Systems accelerometer type OMNIDOTS® [17] was used for the measurement of the vibratory wave signal generated by potential shocks. This choice was made to align with the project's objective of reducing disk storage and energy consumption in embedded systems. The OMNIDOTS® accelerometer prioritizes essential signal features, such as maximal velocity and dominant frequency, over raw signals, thus minimizing storage requirements and enhancing practicality and sustainability in real-world applications. For each instrumented bridge, this sensor was located midspan of the bridge deck's shoulder, as shown in Figure 1. The accelerometer records data in three dimensions, with measurements in the vertical direction (up

**Figure 1**
**Schematic representation of the instrumentation and implementation**

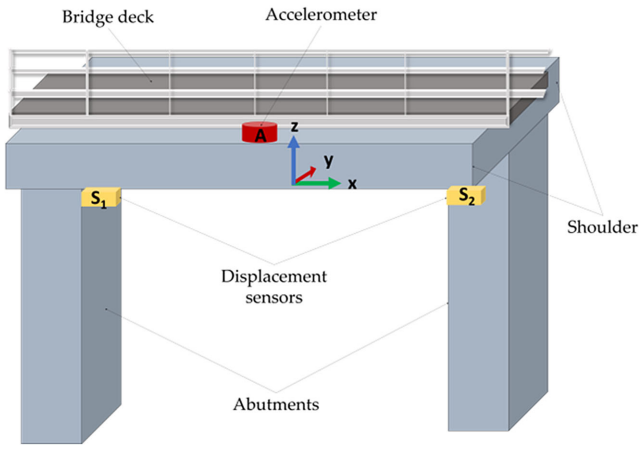


and down), perpendicular direction (left and right), and parallel direction (along the length of the bridge). The accelerometer is equipped with a continuous power supply and connected to a visualization and alerting platform through a 3G/4G connection. In real time, the device provides the dominant frequency and particle velocity of the vibrations based on the user-defined sampling interval, which can range from 2 to 6000 s. The device was securely attached to a solid concrete support, while the power supply battery was fixed near the sensor. The frequency domain covered by the accelerometer ranges between 0.5 and 250 Hz and the resolution of the accelerometer is 1 μm/s.

*2.1.2. Displacement sensors*

The standard Sisgeo® D313 sensor was selected for the measurement of the bridge displacements. One displacement sensor on each side was anchored between the deck abutment and the shoulder of each instrumented bridge, as shown in Figure 1. This sensor uses potentiometric technology and was chosen in this study for (i) the reactivity of the measurement loop without signal conditioning, (ii) its low voltage measurement (reduced power consumption) in a wired configuration, (iii) its large 25 mm amplitude, and (iv) its robust anti-corrosion construction with an IP68 rating. For optimizing the energy consumption, the acquisition time step of the displacement sensors was set up to 30 min. The displacement sensor was intended to complement the accelerometer with measurement of the irreversible displacement the bridges' decks could undergo to enable spotting any permanent changes in the bridge geometry that could indicate a major impact shock.

*2.1.3. Photographic trap*

Due to restrictions associated with installing a video camera in a public space, it was decided to install a camera-trapping device that automatically takes a picture when a high vehicle passes by. This device is powered by a rechargeable battery and solar energy, and its storage disk can be accessed through a remote application. The objective is to use this device to identify the type of vehicle or object that impacted the structure after a collision, assess the potential damage, and link this event to the measurements from the sensors to help calibrate the alert thresholds. The camera traps were positioned to focus on the sub-beam of the deck and do not allow the identification of the vehicle's registration plate.

## 2.2. Monitored bridges

A short list of regularly crashed bridges was extracted from the SNCF-R database for each of which the main structural and geometrical characteristics were accessible. These bridges were selected based on specific criteria, that are (i) accessibility for installation crews, (ii) relatively low height, (iii) heavy truck traffic, (iv) active rail traffic, and (v) a remarkable accident history (frequent collision events).

The study examined four instrumented rail bridges, which are listed in Table 1 along with additional information showing the diversity among selected bridges. One of the bridges, namely Vignacourt (VCT), has been out of service for more than 25 years and was selected in this study to perform a controlled collision experiment to study the effects of shocks with varying energy on the bridge structure. The remaining three bridges, namely Villeneuve Le Roi (VLR), Saint Georges sur Loire (SGL), and Trignac (TRC), were monitored for a one-year period, to provide a dataset for training and validating the ML models.

*2.2.1. Controlled shocks on VCT bridge*

This bridge is composed of a steel deck made of twin beams sustaining the railway tracks directly, and the deck is supported by masonry abutments at each end of the bridge. The metal deck is designed to be lightweight (almost 8 Mg including its equipment). This lightweight construction makes the bridge vulnerable to impacts or shocks. To protect the concrete of the shoulders, a thick piece of wooden protection has been installed on the shoulder prior to the experiment. The goal behind this preliminary experiment is to study the signals that the bridge may encounter and assess the impact of each provoked shock on the bridge's structure. The test involves simulating shocks of increasing energy on the bridge deck using a suspended mass, which is given controlled movement (i.e., varying pendulum angle θ) to generate the desired shock conditions, as shown in Figure 2. Three types of masses were used to analyze the impact the impact material rigidity, including soft contact (a bag full of sand weighing 1.7 Mg), rigid point contact (a demolition ball weighing 1.2 Mg), and large rigid contact (a concrete mass cast in a metal container weighing 2.5 Mg). Multiple shocks of varying energy were applied to the VCT bridge using a lifting crane to hang each mass on $d = 10$ m long. All the data were obtained by the accelerometer ($A$) and the displacement sensors ($S_1$ and $S_2$) located on the bridge.

Figure 3 represents typical acceleration signals obtained with the three different materials. Each mass provided a different signal shape in terms of intensity and damping. However, after analyzing all the signals, it was found that the acceleration toward the $y$ direction (the direction of the shock) was higher than the vertical acceleration of the bridge (in the $Z$ direction) and greater than the velocity in the $X$ direction.

On the other hand, the displacement of the bridge was measured by the displacement sensors. Table 2 represents the displacement registered by the two sensors after each shock. The displacement of the steel deck caused by the impact of different materials ranged from 0.19 to 1.24 mm, depending on the impacting material. For instance, when comparing the impact of a 1.7 Mg sandbag to a 1.2 Mg – metallic ball, the metallic ball was found to have a more harmful effect on the bridge displacement, even with an additional 0.5 Mg. It is important to note that certain impacts can cause the bridge to move in the opposite direction

**Table 1**
**Information about the selected bridges**

| Name of bridge | In service | Structure | Principle material | Length | Number of railway tracks | Reconstruction year | Clearance below bridge |
|---|---|---|---|---|---|---|---|
| VCT | No | Twin beams | Steel | 5 m | 2 | Parior 1950 | 3.32 m |
| VLR | Yes | Pre-stressed concrete beams | Composite steel-concrete | 12 m | 4 | 1987 | 4.3 m |
| SGL | Yes | U-shaped beams reinforced with a concrete shell | Steel | 15 m | 2 | 1991 | 4.3 m |
| TRC | Yes | Coated beam | Composite steel-concrete | 11 m | 2 | 1970 | 4.3 m |

**Figure 2**
**Schematic representation of the experiment performed on VCT bridge**

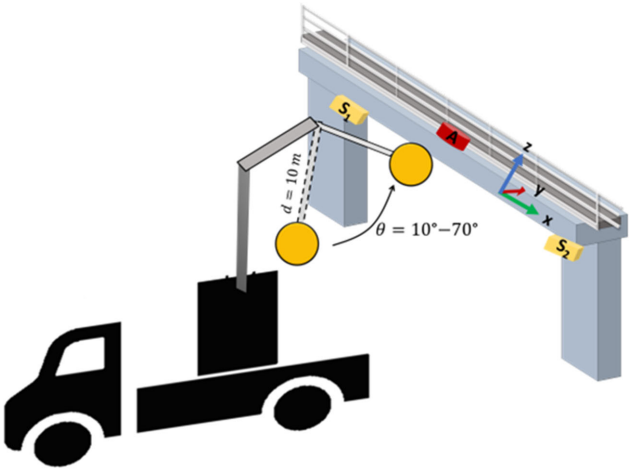


(reversible displacement) due to a strong rebound effect when the shock is intense.

This experiment aimed to investigate the signals resulting from collisions between various materials and a bridge deck, with the objective of gaining a comprehensive understanding. The duration of signal damping was observed to be rapid, occurring within 1–2 s following the impact. Here, the term "damping duration" refers to the time required for the signal to return to its normal state. The acceleration in the *Y* direction exhibited the highest intensity or sometimes approaching the velocity in the *Z* direction, depending on the magnitude of the shock energy. Furthermore, it was determined that a significant shock influenced the displacement of the bridge by at least 0.19 mm. However, it should be noted that the displacement may differ across bridges, as it is contingent upon the specific structure of each individual bridge. This experiment will serve as a valuable tool for classifying and labeling the signals obtained from bridges in active service in the future.

*2.2.2. Bridges in service for monitoring in real conditions*
*Saint George sur Loire (SGL)*

The structure consists of a separate metal U-beam covered with a concrete deck below each railroad track. These decks are protected against collisions by independent heavy shoulders. Although these shoulders are regularly hit, there are no significant signs of displacement. To protect the concrete of the shoulders, a metal angle protector has been installed. The abutments are made of reinforced concrete face wall. In 2017, these decks were structurally reinforced by joining additional plates to enhance their dynamic behavior. Based on the site configuration and the probability of impact assessment, only the north-side shoulder was instrumented.

1) *Villeneuve-le-Roi (VLR)*

The structure of the deck is of the "coated girder" type and is protected by independent heavy concrete shoulders. The abutments are made of masonry. Several frequent incidents have been noted due to the proximity of a waste storage site. Trucks are sometimes loaded beyond the clearance height. The shoulders were lined with metal angle iron, one of which on the west side was destroyed. It is worth mentioning that there are four railway tracks above the bridge.

2) *Trignac (TRC)*

The bridge has a coated beam deck under each railroad track that is frequently hit due to the presence of a nearby concrete plant and some other industrial sites. The deck is relatively heavy and therefore not easily displaceable. Both sides of the bridge (north and south) were instrumented, as the deck has shown signs of repeated impacts in both directions of traffic.

## 2.3. Collected data

*2.3.1. Accelerometer data*

In this study, the acceleration data was not always accessible for all the bridges due to some technical issues with the accelerometer. A software configuration error in the data acquisition process led to a three-month period of missing acceleration data at the beginning of the instrumentation phase. Consequently, it was decided to withdraw the use of acceleration data and instead focus on velocity data, which serves the same purpose. In this study, the data from the TRC bridge will not be considered due to the absence of any signals exceeding the recording threshold, indicating that no major anomalies occurred on this bridge.

Figures 4 and 5 display respectively the velocity and frequency recordings in three directions: *X* (parallel to the track), *Y* (perpendicular to the bridge, in the direction of the vehicle passing under the bridge), and *Z* (vertical to the bridge), for VLR (left) and SGL (right) bridges. The VLR data was collected over a year of monitoring, starting from the day when the sensors were installed (April 4th, 2022 to March 29th, 2023). The bars in Figure 4 represent the absolute maximum velocity detected by the accelerometer for each detected vibration exceeding the threshold value (1 mm/s) in the three different directions. The continuous time series for each observation could be observed by clicking on the bar of each observation. Additionally, the frequency data were obtained by applying a fast

**Figure 3**
**Acceleration of VCT bridge representing three different shocks with 3 different materials**

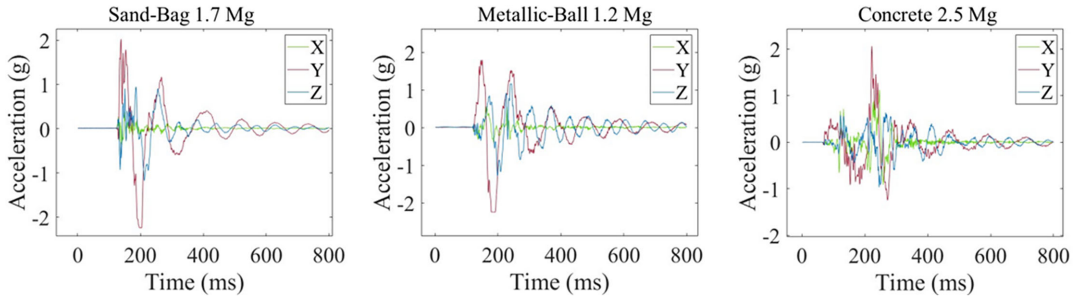


**Table 2**
**The displacement of VCT bridge caused by each shock**

| Material | Sensor 1 (mm) | Sensor 2 (mm) |
|---|---|---|
| Sand bag – 1.7 Mg | 0.26 | 0.19 |
| Metallic ball – 1.2 Mg | 0.55 | 0.69 |
| Concrete – 2.5 Mg | 0.87 | 1.24 |

Fourier transform to the velocity data. Figure 5 (left) represents the dominant frequency in each direction for every detected signal. The dominant frequency represents the frequency component that has the highest magnitude or contributes the most to the overall velocity signal. The dominant frequencies are found to be ranging between 1 to 60 Hz in all directions. It's important to mention that the continuous time series velocity data will be used for the signal and features analysis part, while only significant features of these signals (consisting of the maximum velocity values and dominant frequency values in the *X*, *Y*, and *Z* directions) will be used for the model training section. After one year of monitoring the bridge, 100853 signals were recorded by the accelerometer (equivalent to over 200 trains passing over the bridge each day). However, the signals may vary in velocity intensity depending on factors such as the mass and velocity of the train as well as the rail track it passes on. Upon reviewing the maximal velocity values presented in Figure 4, several outliers could easily be observed.

Moreover, the SGL data were collected over a year of monitoring, starting from the day when the sensors were installed (April 16$^{th}$, 2022 to March 29$^{th}$, 2023). The behavior of SGL bridge was found to be similar to that of the VLR bridge, as both have exposed an average velocity ranging between 1 and 10 mm/s, under usual train passages. Besides, the dominant frequencies range between 1 to 80 Hz in all directions. While examining the velocities obtained by SGL bridge, at least one clear outlier could be observed in all three directions. Overall, a total of 27303 signals were recorded by the accelerometer, with at least one or two outliers observed. However, these outliers may have been caused by a sensor defect or other reasons that do not significantly affect the bridge structure. Therefore, to validate the nature of these outliers, further examination of the displacement sensor outputs is required.

*2.3.2. Displacement*

Figure 6 (left) illustrates the displacement of VLR bridge recorded by the two displacement sensors over one year of monitoring. The figure displays several distinct displacements ranging between 0.01 to 1.57 mm. Additionally, there were instances where displacement was detected solely by one sensor, depending on the direction of the vehicle's passage. Certain significant displacements occurred but were unobserved by the accelerometer. For instance, on 31th October 2022, a clear displacement was observed by the displacement sensor, while no corresponding vibration was detected by the accelerometer at the same time. This discrepancy could be attributed to a defect or inaccurate estimation by one of the sensors.

Figure 6 (right) presents the displacement of SGL bridge. Several minor displacements with a magnitude of less than 0.03 mm are observed frequently (i.e., more than 3000 instances), and this is believed to be produced by train passages. Additionally, the figure also confirms the presence of an anomaly that was already identified by the accelerometer on March 11$^{th}$, 2022. This displacement, which exceeded 1 mm and had a very high velocity value at the same time, demonstrates the consistency between the two sensors.

Due to solar charging issues, the sensors were temporarily out of service for a specific duration. For the VLR bridge, the sensors were out of service from December 26$^{th}$, 2022 to January 26$^{th}$, 2023, as depicted in Figure 6 (between the two vertical lines), where no changes in bridge displacement were observed during this period. Similarly, the sensors on the SGL bridge also experienced the same issue and were out of service between January 15$^{th}$, 2023 and March 15$^{th}$, 2023. Due to the inaccessibility of data during these periods, it will be excluded from consideration in this study.

## 3. Data Preprocessing

Data preprocessing focuses on the required tasks to prepare the dataset for accurate analysis and modeling. In this section, key aspects such as threshold determination for anomaly detection, data cleaning, synchronization, signal pattern identification, data labeling, statistical feature extraction, and data partitioning for training and testing the ML model are addressed. These preprocessing steps are essential for ensuring the quality, reliability, and suitability of the data for subsequent analysis.

### 3.1. Threshold determination for anomaly detection

Choosing an appropriate threshold value for anomaly detection problems is a critical step in creating an effective model. In this section, the significance of the threshold value in detecting and categorizing signal types is discussed. The structures of the studied bridges differ, and the behavior of each of them is unique; thus, a single threshold value for all bridges may not be optimal for detecting anomalies. Therefore, it is important to choose an

**Figure 4**
**The absolute maximal velocity of VLR (left) and SGL (right) over one year of monitoring**

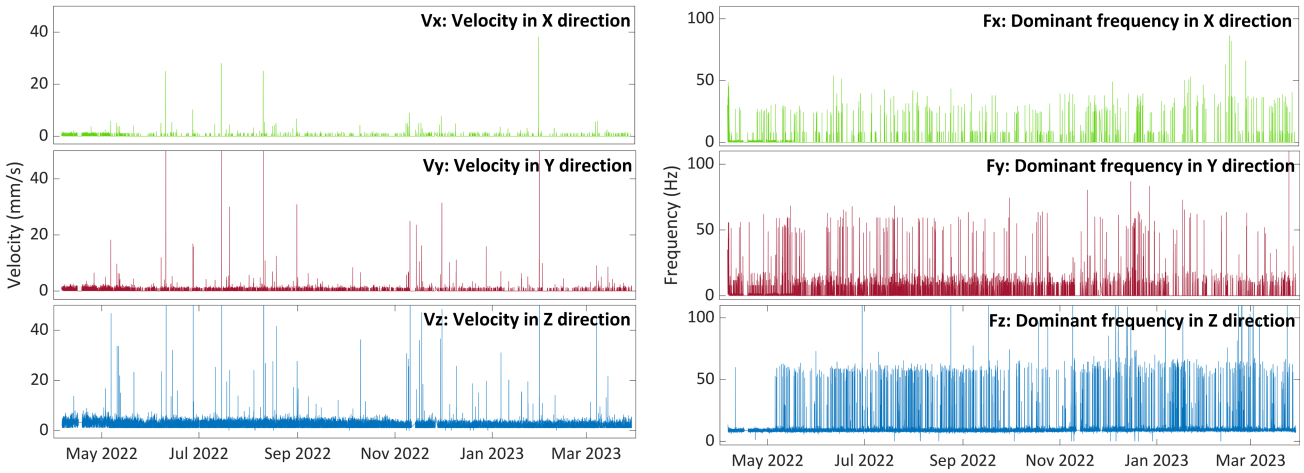


**Figure 5**
**The dominant frequency of VLR (left) and SGL (right) over one year of monitoring**

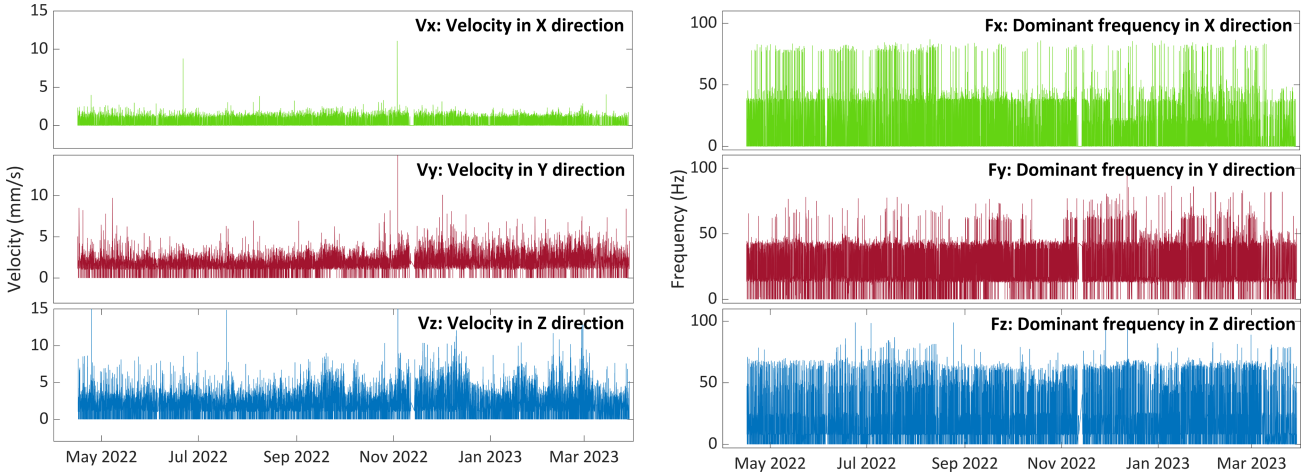


appropriate specific threshold value for each bridge to ensure that the model will be accurately capturing the anomalies depending on each bridge's behavior.

A statistical approach is employed to calculate threshold values based on a representative sample of signals associated with normal train passages. Considering VLR bridge, a reference sample of 200 train signals without shocks was manually selected. Based on this reference sample, the threshold value for each direction was determined by adding the standard deviation to the maximum velocity observed in the reference sample for that direction. The inclusion of the standard deviation in the threshold calculation is motivated by the analysis of the data, which revealed that certain subsequent normal train passages exhibited velocities slightly higher than the maximum value obtained from the sample of 200 trains. Incorporating the standard deviation ensures that the threshold accounts for potential variations and enables differentiation between normal train passages and anomalies. Hence, the threshold value in $X$ direction is $TZ = 1.9$ mm/s and is calculated as the maximum velocity observed in the $X$ direction in the reference sample plus the standard deviation. Similarly, $T_Y = 2.9$ mm/s and $T_Z = 9.1$ mm/s denote the threshold values for the $Y$ and $Z$ directions, respectively. A signal is classified as an anomaly when it exceeds the predetermined threshold values in both the $Y$ and $Z$ directions simultaneously (i.e., $V_Y > T_Y$ and $V_Z > T_Z$). It is important to note that certain anomalies may exhibit velocities in the X direction below the threshold value (i.e., $V_X < T_X$). However, the performed analyses revealed that, to identify an anomaly, it is sufficient for the velocities in the $Y$ and $Z$ directions to surpass the threshold values. The $X$ direction velocity provides additional contextual information but does not play a significant role in the anomaly detection process.

Further analysis revealed that out of the total signals, only 65 signals exceeded the threshold values. Detailed examination confirmed these signals as anomalies not associated with normal train passages, which will be addressed in Section 3.3. The effectiveness of the presented approach is demonstrated by its ability to accurately differentiate between train passage signals and anomalous signals, resulting in a satisfactory overall analysis

**Figure 6**
**The bridge displacement of VLR (left) and SGL (right) bridges during one year of monitoring**

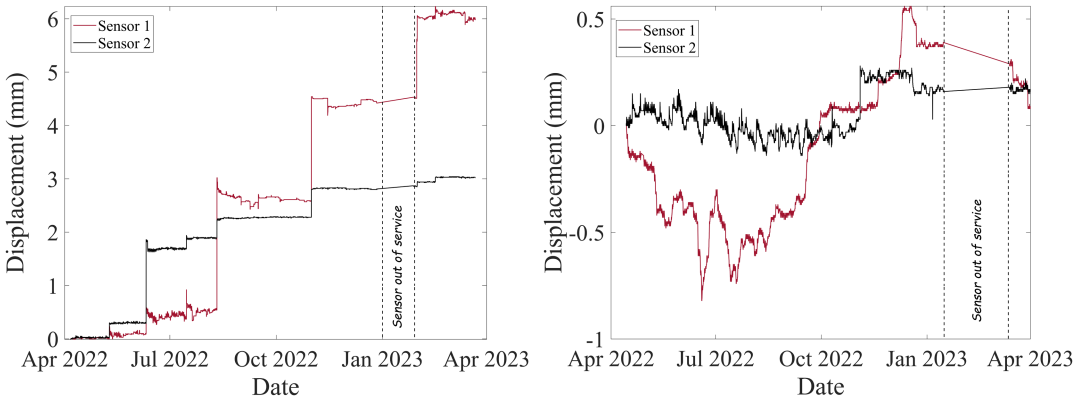


accuracy. The same procedure was applied to the dataset obtained from the SGL bridge, where the threshold values were determined as follows: $T_X = 2.05$ mm/s, $T_Y = 6.07$ mm/s, and $T_Z = 7.22$ mm/s. Consequently, out of the total signals, only 8 signals exceeded the threshold values in the $Y$ and $Z$ directions.

## 3.2. Cleaning and synchronization

Data cleaning is an essential step in ensuring the quality and reliability of data collected from sensors installed on railway bridges. This process involves identifying and removing missing values or erroneous measurements that may arise during data acquisition. In this study, data cleaning step was performed on all data to eliminate any discrepancies that could potentially affect the classification of vehicle-deck collisions.

As an initial step in the data cleaning process, signals exhibiting a velocity less than 1 mm/s are promptly excluded before undergoing evaluation by the ML model. The determination of this threshold for measurement retention draws upon the experiential insights of the managing staff (SNCF-R). This criterion serves to eliminate noisy and inconsequential data, ensuring the quality and relevance of the retained dataset.

Section 2.3.2 of the article addressed the solar charging issues encountered during the remote monitoring of the bridges. These issues resulted in the displacement sensors going out of service, leading to missing displacement data. Since the classification decision in this study relies on data from both sensors, it is necessary to neglect the accelerometer data obtained when the displacement sensors were turned off. This ensures that only reliable and synchronized data from both sensors are utilized for the classification analysis.

Furthermore, the synchronization of the three sensors used was conducted to validate the cause of the high-intensity signals. During the synchronization process, it was observed that the accelerometer and the displacement sensors were well synchronized in terms of time. However, when examining the camera trap, numerous photos were not captured at the exact moment of the detected velocity vibration and displacement. This issue with the camera trap was attributed to solar charging problems, which led to dyssynchronization between the camera trap timer and the timer of other sensors. Some of the high-intensity signals could be validated by a camera trap, as illustrated in Figure 7. The figure depicts an example where the collision between the vehicle and the bridge was confirmed by all three sensors on July 15, 2022. The left picture shows the truck that collided with the bridge, while the middle figure displays the displacement of the bridge after the collision, recorded as $S_1 = 0.55$ mm and $S_2 = 0.25$ mm. On the right side of the figure, the vibratory signal representing the velocity of the bridge caused by the shock can be observed, exhibiting high intensities in all directions, surpassing the threshold values presented in Section 3.1.

## 3.3. Signal patterns identification

Upon analyzing the acquired signals, our investigation revealed three distinct categories: normal train passages, major impact anomalies indicative of harmful vehicle/bridge collisions, and unidentified anomalies.

### *3.3.1. Normal train passage*

In Section 2.2.1, controlled shocks were conducted on the VCT bridge using varying energy levels to observe the bridge's response and evaluate the structural effects. The analysis of the results provided valuable insights into how detrimental shocks influence the bridge displacement and velocity. This section focuses on studying the signals generated by a train crossing the VLR bridge and their impact on the displacement. To carry out this investigation, the VLR bridge was closely monitored for 4 h by a technical team to study the signals recorded as 40 trains were crossing the bridge. Figure 8 shows the signals of trains passing on different tracks. To ensure clear visualization and prioritize the most important signal features during a train passage, only the velocity in the $Z$ direction is displayed. The analysis revealed that the velocity ranged between 1 mm/s and 8 mm/s and the displacement caused by a train did not exceed 0.03 mm. Peaks of signals caused by a train were characterized by a short period (30 to 100 ms), distinguishing them from shock-induced signals recorded during the controlled experiment on the VCT bridge (Figure 3). The track on which the train passes does not significantly affect the signal, as all signals from different tracks exhibit similar characteristics. However, the range of maximum velocity and the dominant frequency for a train passage may differ for another bridge depending on the bridge structure. Factors such as train mass, length, and speed may influence the signal, although they do not significantly adjust its shape or intensity. Instead, they can cause the sensor to detect the signal for a longer period.

**Figure 7**
**A vehicle/ bridge collision validated by all three sensors installed on the VLR bridge. Trap camera (left), displacements (middle), and velocity (right)**

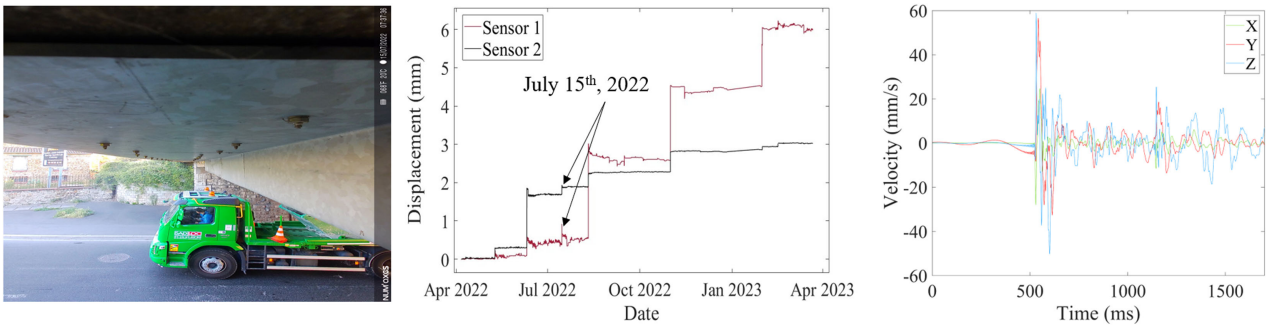


*3.3.2. Anomaly categories*

After conducting a thorough analysis of the obtained signals, our study revealed the presence of two distinct types of anomalies, namely Major Impact anomalies and Unidentified anomalies.

1) *Major Impact anomaly*

These signals represent the velocity induced by a heavy or harmful vehicle/bridge collision, impacting the bridge's structural integrity. Figure 9 illustrates an example of a major impact anomaly that occurred on VLR bridge on August 10, 2022. The period of these signals (140 to 200 ms) differs significantly from normal train passages, and a notable displacement exceeding 0.1 mm is observed. Additionally, the velocity intensity is higher than 7.9 mm/s, which is the velocity threshold for train passages on VLR. Furthermore, the velocity in *Y* direction is higher than in the *Z* and *X* directions, which is consistent with the results provided by the first approach (controlled shocks) presented in Section 2.2.1.

2) Unidentified anomaly

While monitoring the VLR bridge for four hours, an unexplained signal with high intensity exceeding 11 mm/s was detected, without any train passage or serious anomaly (Figure 10). The cause of this signal could be attributed to several factors surrounding the bridge, including environmental conditions, nearby construction activities, or traffic. No significant change in bridge displacement was registered during these events. While examining the available data over one year of the VLR bridge monitoring, this type of signal was detected frequently with no apparent impact on the bridge displacement. Thus, an additional category of signals must be considered to account for what will be referred to as "Unidentified anomaly" that does not affect the structure of the bridge. These signals may be produced by an unusual train configuration, light vehicle friction with the bridge, environmental conditions, or nearby construction activities surrounding the bridge.

In conclusion, this systematic approach to signal pattern identification involved closely monitoring the VLR bridge and conducting controlled experiments to visualize the effects of real shocks compared to train passages. This allowed us to distinguish between train signals and anomaly signals (e.g., velocity and displacement thresholds, and signal periods), leading to the discovery of a new pattern that does not belong to either category as it has the pattern of an anomaly but does not influence the bridge structure as a major shock.

**Figure 8**
**The signals in *Z* direction of four different trains passing on different tracks (*T*1, *T*2, *T*3, and *T*4) above VLR bridge**

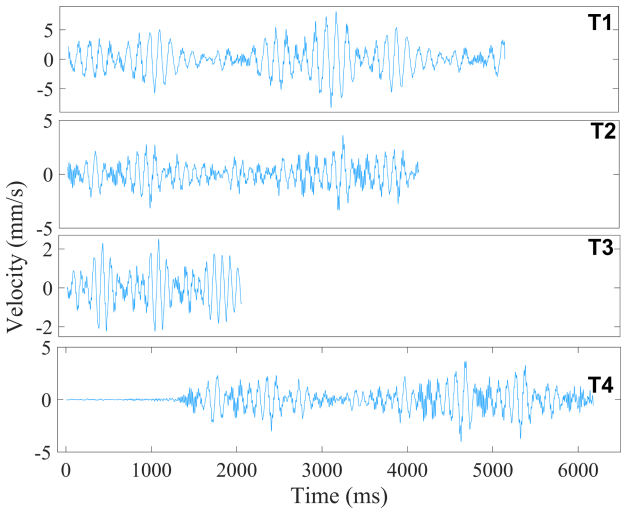


## 3.4. Data labeling

The accelerometer and displacement sensors are essential devices that provide valuable contextual information. Each bridge has its unique characteristics, which can affect its behavior. In this section, the data obtained by the accelerometer and displacement sensor is used to distinguish 3 different types of signals.

After applying predetermined threshold values to the VLR and SGL bridge dataset, the signals were classified into two categories: train passages and anomalies. In the VLR dataset, out of a total of 100853 signals, 100788 were identified as train passages, while 65 signals were classified as anomalies. Similarly, in the SGL dataset, out of 27303 signals, 27295 were identified as train passages, with only 8 signals detected as anomalies. These results were validated and demonstrate the effectiveness of the applied thresholds in accurately distinguishing between normal train passages and anomalies in both datasets. Afterward, the 65 anomaly signals found in the VLR dataset underwent further analysis to classify them as either major or unidentified anomaly. Despite the presence of high amplitude signals from the accelerometer data (Figure 4), it is difficult to determine whether a given signal indicates a major or an unidentified anomaly. While some camera pictures were

**Figure 9**
**Example of a major impact anomaly signal produced by a vehicle/bridge collision on VLR bridge on August 10th, 2022**

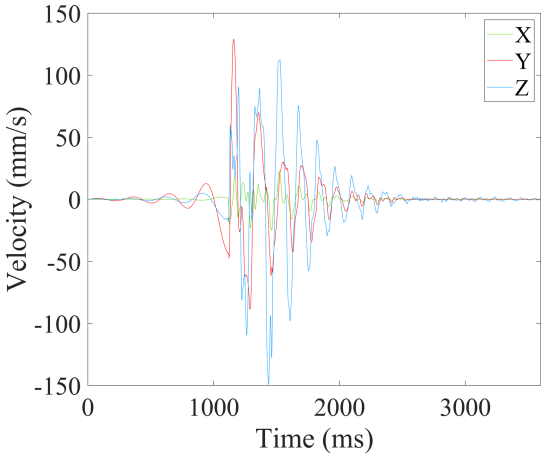


**Figure 10**
**Unexpected signal detected while remoting the bridge during the presence of our team beside the bridge**

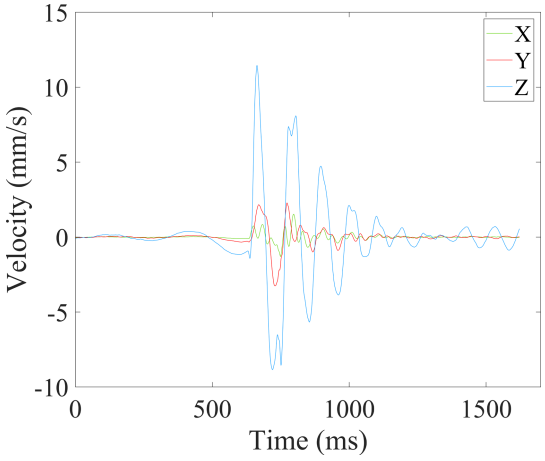


available, others were not found due to a lack of solar power and temporal desynchronization, making them unreliable for identifying the cause of the high amplitude signals.

Thus, to identify a major impact anomaly that influenced the bridge structure, the displacement data is used and compared with the accelerometer outputs. If both displacement and velocity of bridge surpass the threshold values (i.e., the displacement threshold value is considered as 0.1 mm), then the signal will be considered a major impact anomaly; otherwise, it will be considered an unidentified anomaly.

**Table 3**
**The label of all recorded signals by both bridges VLR and SGL**

| Bridge | Normal train passage | Major impact anomaly | Unidentified anomaly |
|---|---|---|---|
| Villeneuve Le Roi | 100788 | 7 | 58 |
| Saint George sur Loire | 27295 | 1 | 7 |
| Total | 128083 | 8 | 75 |

To enhance the reliability of distinguishing major and unidentified anomalies, the threshold was judiciously chosen based on experimental data gleaned from controlled shocks on the VCT bridge. These controlled experiments simulated major shocks, and the observed displacement during these controlled shocks serves as a robust reference point. The chosen threshold of 0.1 mm reflects a conservative approach, ensuring safety by considering that the minimum displacement caused by a major shock during controlled experiments was observed to be 0.18 mm. This safety margin accommodates potential variations and uncertainties in real-world scenarios. Moreover, the threshold selection aligns with engineering practices and standards, encompassing a blend of empirical observations, expert judgment, and safety considerations. This approach ensures that the model's classification decisions are not only robust but also prioritize safety considerations.

The illustration of the labeling algorithm is presented in Figure 11 and the labeling of all recorded signals by both bridges is presented in Table 3. The results of the analysis indicated that out of the 65 signals, 7 were identified as major anomalies, while the remaining 58 signals were classified as unidentified anomalies. The same analysis was also performed on the SGL dataset, revealing that only one of the 8 anomalies represented a major impact anomaly, whereas the remaining 7 anomalies were classified as unidentified anomaly.

In the next section, multiple ML algorithms will be applied to classify all the different types of signals. It is worth mentioning that the velocity data were normalized for two reasons. The first reason is that the same model is intended to be used for all bridges, and it should then be able to detect and classify signals obtained from any bridge, since the velocity of each bridge differs from the

**Figure 11**
**Illustration of labeling algorithm**

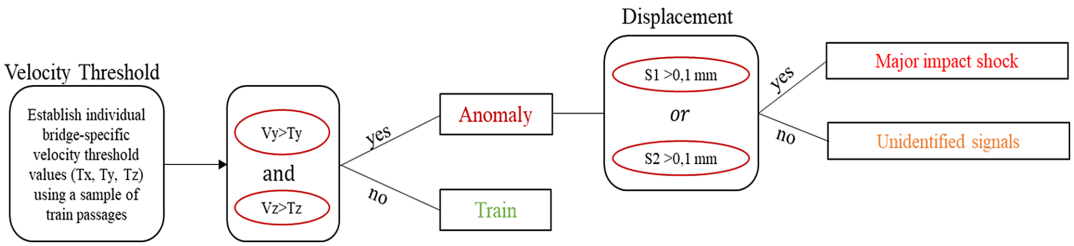

others depending on its structure, train speed, and mass above it. Therefore, the velocity data will be normalized by dividing the maximum velocity of each signal by the corresponding threshold value. Specifically, $V_{X\text{-}Norm} = V_X/T_Y$ mm/s, $V_{Y\text{-}Norm} = V_Y/T_Y$ mm/s, and $V_{Z\text{-}Norm} = V_Z/T_Z$ mm/s.

### 3.5. Statistics and feature extraction

Before implementing a supervised model, it is essential to apply feature selection algorithms to enhance the model's accuracy and efficiency. Furthermore, feature selection methods can offer valuable insights into the significance of the features in the dataset. Three feature selection methods, namely MRMR [18], Chi2 [19], and Kruskal-Wallis [20], are applied to the 6 features $V_X$, $V_Y$, $V_Z$, $F_X$, $F_Y$, and $F_Z$. The MRMR method assesses the relevance and redundancy of each feature by calculating mutual information between the feature and the target variable, as well as between each feature and every other feature. It provides a comprehensive evaluation of feature importance. The Chi2 method tests the independence between two variables and determines whether they are statistically dependent or independent. This method is particularly useful for categorical or discrete variables. Lastly, the Kruskal-Wallis method tests whether the distribution of a numerical variable significantly differs across distinct groups, making it suitable for identifying features with significant variations among different categories or groups. By applying these feature selection methods, valuable insights can be gained into the importance and relevance of the features, ensuring that the selected features contribute meaningfully to the subsequent classification analysis. The results obtained by the three methods are presented in Figure 12.

After analyzing the results, the following observations were reported:

Regarding MRMR, $V_Y$ exhibited the highest MRMR score, indicating its significance as the most informative feature for discriminating between the target variable classes. $V_X$ and $V_Z$ also demonstrated high MRMR scores, indicating that they are also informative features for discriminating between the classes. For Chi2, $V_X$ and $F_X$ were found with the highest scores, indicating a strong association with the target variable. Additionally, $V_Y$, $V_Z$, and $F_Y$ exhibited noteworthy scores, suggesting their informative characteristics for the classification process. In the case of Kruskal-Wallis, $V_X$ and $F_X$ obtained the highest scores, implying significant differences in their distributions across the target variable groups. $V_Y$, $V_Z$, and $F_Y$ also received high Kruskal-Wallis scores, further highlighting the dissimilar distributions among the groups. Overall, the results from the three feature selection methods provide different perspectives on the importance of the features. Kruskal-Wallis and Chi2 suggest that $V_X$ and $F_X$ are strongly associated with the target variable, while $V_Y$ and $F_Y$ have distributions that differ significantly across the groups. MRMR suggests that $V_Y$ is the most informative feature for discriminating between the groups, followed by $V_X$ and $V_Z$. It is worth noting that $F_Z$ demonstrated negligible importance based on the scores obtained from all three algorithms. Based on these comprehensive results, it would be reasonable to retain only five features for training the classification model, excluding $F_Z$ from consideration.

### 3.6. Data partitioning (Training/Testing)

As mentioned previously, to create a model that can be generalized to any bridge, all the velocity data should be normalized using the threshold values calculated in Section 3.1. This allows to account for differences in the structure of each bridge and ensures that the model is not biased toward a specific bridge. After normalizing all the velocity data, 75% of the data obtained by both bridges (VLR and SGL) will be trained in order to create the model that detect and categorize the type of each tested signal from the remaining 25% data. It is worth mentioning that the data partitioning was performed in a random manner and repeated multiple times to ensure robustness of the models. This means that the models were trained using various forms of data partitioning, ensuring the presence of sufficient data representing both unidentified and major anomalies throughout the testing process. Therefore, this study will present one of the examples that reviews the most crucial aspects to be discussed and summarizes the various possibilities that may be encountered.

## 4. Model Development

The performances of the ML methods were investigated using the parameters accuracy, precision, recall, and $F1$-score, which are determined from the confusion matrix. In this study, the signals provided by the bridge are being attempted to be classified, thus the problem is regarded as a supervised classification problem. The four algorithms that are employed in this study are:

1) **Random Forest (RF):** RF [21] is an ensemble learning method that constructs multiple decision trees during training and combines their predictions through a voting mechanism to determine the final classification. It is highly effective for

**Figure 12**
**Feature importance scores using MRMR, Chi2, and Kruskal-Wallis algorithm**

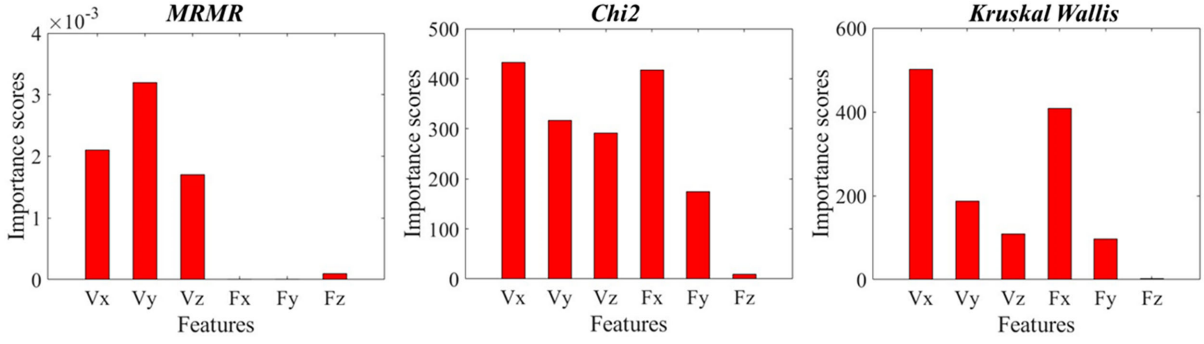

**Figure 13**
**Confusion matrices obtained using the tested data for RF, KNN, ANN, and SVM models, from left to right**

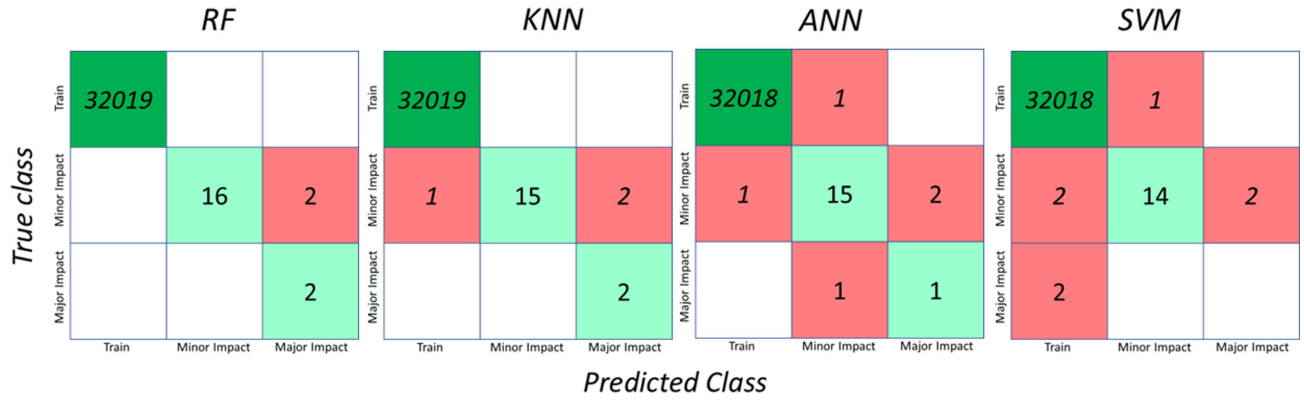


classification tasks due to its ability to handle high-dimensional data and its robustness to overfitting.

2) **K-nearest neighbors (KNN):** KNN [22] is a non-parametric method used for classification by determining the majority class of its k nearest neighbors in the feature space. It is particularly suitable for classification tasks where the decision boundaries are complex or non-linear.
3) **Artificial Neural Network (ANN):** ANN [23] is a computational model inspired by biological neural networks, capable of learning complex patterns in data. It is well-suited for classification problems, especially when dealing with large datasets and non-linear relationships between features.
4) **Support Vector Machine (SVM):** SVM [24] is a powerful supervised learning algorithm for classification tasks. It constructs hyperplanes in a high-dimensional feature space to separate classes with maximum margin. SVM is effective for classification tasks with complex decision boundaries and is known for its versatility in handling various types of data.

The performance of these algorithms is evaluated for classifying the three categories: normal train passage (A), unidentified anomaly (B), and major impact anomaly (C). Figure 13 displays the confusion matrices for RF, KNN, ANN, and SVM models, from left to right. It is worth noting that all the algorithms underwent hyperparameter optimization to maximize their performance to achieve the best possible results.

The optimal hyperparameters for the RF model were determined through a systematic hyperparameter tuning process. A grid search technique was employed to explore different combinations of hyperparameters, including the number of learners (representing the number of decision trees in the forest ensemble) and the maximum number of splits. After evaluating the performance of various hyperparameter configurations using cross-validation, the optimal settings were identified as 295 learners and a maximum number of splits set at 4561. This model exhibited a high level of accuracy, achieving a true positive rate of 100% for class A instances and 88.88% for class B instances, with a perfect classification rate of 100% for class C.

Similarly, the KNN hyperparameter tuning process was configured to employ 1 neighbor and the Euclidean distance metric. This optimized configuration resulted in a high accuracy across all classes, with the model achieving a true positive rate of 100% for class A, 83.33% for class B, and 100% for class C.

For the ANN model, the hyperparameter tuning process identified the optimal configuration, which includes two hidden layers. The first hidden layer comprises 286 nodes, while the second layer comprises 61 nodes, both employing a sigmoid activation function. Stochastic Gradient Descent was utilized to optimize the learning parameters (weights and biases) of the ANN model, ensuring efficient convergence and improved performance in classifying the data accurately. This model achieved a true positive rate of 99.99% for class A, 83.33% for class B, and 50% for class C.

For the SVM model, the hyperparameters were tuned using a grid search method. The tuning process identified the optimal configuration, which consisted of a Quadratic kernel function, the one-vs-one multiclass method, a box constraint level of 300, and a kernel scale of 5. The SVM model achieved a true positive rate of 99.99% for class A, 77.78% for class B, but did not identify any instances of class C, resulting in a true positive rate of 0% for that class.

Table 4 summarizes the results obtained by the tested data using the supervised ML methods. It shows that all the algorithms gave excellent results with an accuracy = 99.99%. However, RF was found with the highest precision = 99.997%, and highest recall = 99.994%, and *F*1-score = 99.995% compared to all other algorithms.

## 5. Results and Discussion

Based on the results provided in the previous section, each of the four models performs well in classifying the data under different impact scenarios. However, each model has its strengths

**Table 4**
**Classification report for the supervised machine learning methods**

| Method | Accuracy (%) | Precision (%) | Recall (%) | *F*1-score (%) |
|---|---|---|---|---|
| Random forest | 99.993 | 99.997 | 99.994 | 99.995 |
| Kth nearest neighbor | 99.990 | 99.986 | 99.990 | 99.988 |
| Artificial neural network | 99.977 | 99.979 | 99.977 | 99.978 |
| Support vector machine | 99.971 | 99.980 | 99.971 | 99.975 |

**Figure 14**
**The signals predicted as major impact anomalies: October 18th, 2022 (left) and November 30th, 2022 (right)**

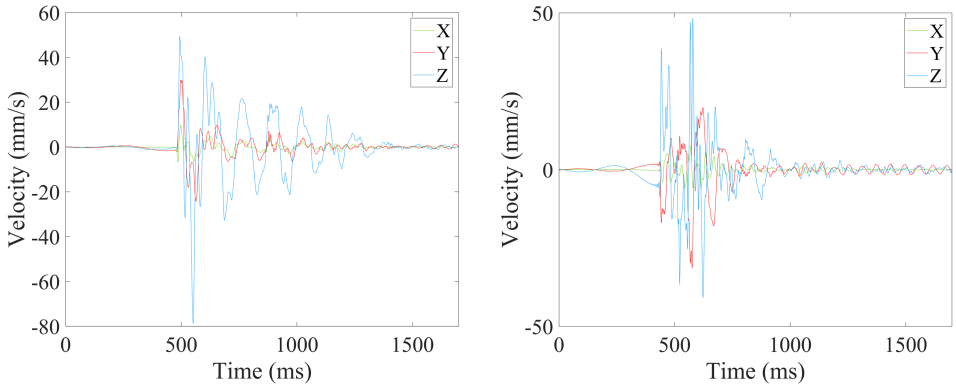


and weaknesses, and the choice of the best model depends on the bridge manager's specific target.

For the "Normal Train Passage" scenario, all models achieved high true positive rates, with the RF model exhibiting a rate of 100%, closely followed by KNN (100%). However, ANN and SVM failed to identify one instance of class A, resulting in a true positive rate of 99.99%.

When it comes to classifying "Unidentified Anomaly," the RF model demonstrated the highest true positive rate of 88.89%, indicating its effectiveness in accurately identifying these instances. Both KNN and ANN models achieved a true positive rate of 83.33% for class B, showing comparable performance. However, the SVM model exhibited a slightly lower true positive rate of 77.78% for class B, suggesting some challenges in accurately distinguishing unidentified anomaly. These results emphasize the superior performance of the RF model in correctly classifying unidentified anomaly, followed closely by KNN and ANN models.

Regarding the "Major Impact Anomaly" (class C), the RF and KNN models achieved a perfect true positive rate of 100%, indicating their effectiveness in accurately identifying instances of this class. The ANN model exhibited a true positive rate of 50% for class C, suggesting challenges in accurately distinguishing major impact anomalies. On the other hand, the SVM model had a true positive rate of 0% for class C, indicating that it did not correctly predict any instances of this class. These findings highlight the superior performance of the RF and KNN models in identifying major impact anomalies, while the ANN model showed some limitations in this specific scenario.

Based on the analysis performed on the confusion matrices, it was evident that all the models misclassified two unidentified anomaly instances as major impact anomaly. Further investigation into these specific instances revealed that all the models identified the same two signals. This prompted a closer examination of these ambiguous cases. Figure 14 illustrates the two signals detected on October 18 2022, and November 30 2022, both occurring on the VLR bridge, which were predicted as major impact shocks by all the models. Notably, both signals exhibited high intensities exceeding 40 mm/s in the $Z$ direction and 25 mm/s in the $Y$ direction. This observation clarifies why the models predicted these two signals as major impact shocks.

In this study, the major impact anomalies were labeled based on the displacement values that exceeded 0.1 mm following an anomaly. Upon analyzing the displacement induced by these two occasions, it was found that the displacement values for the signal on 18th October were $S_1 = 0.03$ mm and $S_2 = 0$ mm, whereas for the signal on 30th November, the values were $S_1 = 0.03$ mm and $S_2 = 0.01$ mm. As mentioned earlier, the displacement sensor recorded data at 30-minute intervals. Therefore, there may be some instances where the bridge rebounded to its initial position, resulting in displacement values that did not fully reflect the instantaneous impact on the bridge. These two examples seem to demonstrate such cases and should be considered as major impact anomalies as proposed by the models.

Furthermore, upon examining the confusion matrices generated by KNN, ANN, and SVM, it was noticed that all three models misclassified an unidentified as a normal train passage. A more detailed investigation into this particular signal revealed that the models consistently misclassified the same signal, which occurred on March 27, 2023, at the SGL bridge. Figure 15 presents this velocity signal, which was incorrectly classified as a normal train passage by the models. Based on the signal pattern identification criteria discussed in Section 3.3, it is evident that this signal does not correspond to a normal train passage. The models KNN, ANN, and SVM misclassified the signal due to the presence of a low maximal velocity in the $X$ direction, $V_X = 1.04$ mm/s, leading the models to mistakenly classify it as a train passage signal. This example reinforces the choice made to neglect the velocity in the $X$ direction while labeling the data in Section 3.4.

**Figure 15**
**The misclassified signal of March 27th, 2023 at the SGL bridge**

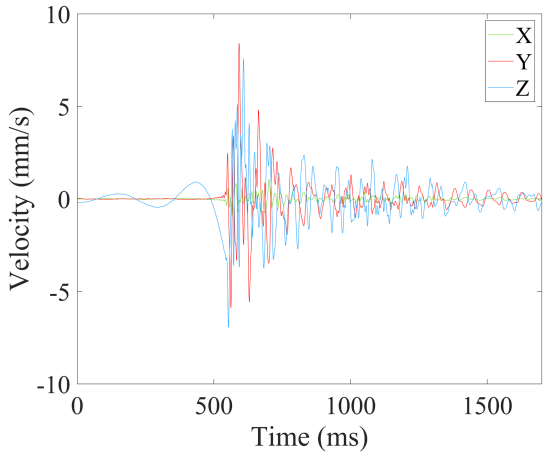

**Figure 16**
**The velocity signal from April 21th, 2022, at the VLR bridge**

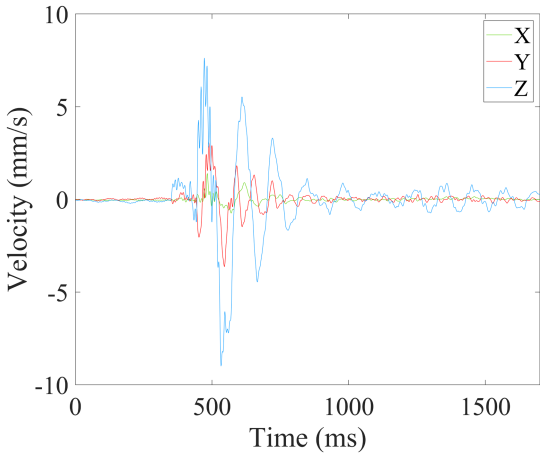


Moreover, a particular signal that was already labeled as a train passage (based on the threshold calculation discussed in Section 3.1) was misclassified by ANN and SVM models as an unidentified anomaly. Figure 16 presents the velocity signal from April 21, 2022, at the VLR bridge, which was incorrectly classified as a normal train passage by ANN and SVM. However, based on the signal pattern identification Section 3.3, it is evident that this signal does not correspond to a normal train passage. This discrepancy raises concerns regarding the performance of the ANN and SVM models and contradicts the results obtained by applying the calculated threshold. To further understand the reason behind the misclassification, it is important to analyze the maximum velocity values of this signal in the $Y$ and $Z$ directions. These values need to exceed the thresholds $T_Y$ and $T_Z$, respectively, to classify a signal as an anomaly. However, the maximum velocity in the $Z$ direction was found to be 8.99 mm/s, which is below the threshold value of $T_Z$ = 9.1 mm/s. Consequently, since the maximum value in the $Z$ direction fell below the threshold, this signal was classified as a train passage. This misclassification highlights the importance of carefully choosing the threshold value in anomaly detection. The threshold serves as a crucial parameter in distinguishing between normal train passages and anomalies. In this case, even a slight deviation of 0.11 mm/s from the threshold value resulted in an incorrect classification.

Therefore, it is imperative to consider the unique characteristics of the signals and set an appropriate threshold that accounts for possible variations in the data. This ensures the accuracy and reliability of the anomaly detection process. Based on the obtained results, the RF model demonstrated superior accuracy compared to the other three models. Notably, only the RF model was capable of correctly identifying the signal detected from the SGL bridge on March 27$^{th}$ as an anomaly. Moreover, the RF model exhibited the highest precision, accuracy, recall, and $F$1-score among all the models evaluated.

However, it is important to note that some instances were misclassified by the models. Specifically, the signals from October 18, 2022 to November 30, 2022 were labeled as a major impact anomaly by all the models, despite their initial classification as an unidentified anomaly. On the other hand, the displacement sensors revealed a 0.5 mm and 0.4 mm displacement for both events, respectively, which is less than the chosen threshold value (0.1 mm). This finding emphasizes the limitations of relying solely on displacement measurements for precise anomaly classification.

As mentioned previously, the careful selection of the threshold ensures that the model's classification decisions are not only robust but also prioritize safety considerations. Therefore, for safety reasons, the final model is trained considering the two misclassified signals as major impact shocks. This precautionary approach reflects the importance of prioritizing safety in anomaly detection, even if it means classifying certain signals conservatively to avoid potential risks or oversights. Additional factors or features, beyond displacement, may need to be considered to improve the accuracy and reliability of anomaly classification in such cases.

## 6. Conclusion

This study represents a pioneering effort in the development of a ML-based monitoring system specifically designed to detect and classify vehicle/deck collisions on railway bridges. Unlike previous research that predominantly focused on the effects of trains passing over bridges, our work is the first to address the critical issue of collisions beneath the bridge structure. The proposed approach achieves an accuracy of 100% in detecting vehicle-deck collisions and has the potential to significantly improve the safety and reliability of railway bridges by providing early warning of potential collisions and allowing for proactive maintenance and timely interventions to address structural damage. Moreover, the development of a real-time monitoring system using the proposed approach can enhance the efficiency and effectiveness of bridge management practices, while reducing disk storage requirements and energy consumption.

The main objective of this study was to develop a generalized model applicable to various bridge structures and dimensions, surpassing the limitations of previous studies that focused on specific bridges. To achieve this aim, extensive data preprocessing was conducted as a crucial step before training the classification model. Challenges associated with selecting appropriate threshold values for accurate data labeling were effectively addressed. The cleaning and synchronization processes successfully tackled missing data and asynchronization issues observed among the sensors. Additionally, three feature selection methods were employed to establish the significance of features in the dataset, revealing that $F_Z$ demonstrated negligible importance, and thus, it was excluded from consideration. Signal pattern identification was conducted through two experimental approaches aimed at distinguishing between train passage signals and anomalies. These approaches involved monitoring the bridge during train passages in the presence of the technical team, as well as simulating controlled shocks on an out-of-service bridge using a suspended mass.

Following the data preprocessing stage, several supervised ML algorithms, namely KNN, SVM, RF, and ANNs, were trained and compared in order to identify the model with the highest accuracy for detecting vehicle-deck collisions in railway bridges and assess their influence of the structure. The RF model demonstrated the highest accuracy in classifying the signals obtained from the bridges. This model successfully categorized all tested signals, showcasing its effectiveness in identifying significant anomalies that could influence the structural integrity of the bridge. However, it occasionally misclassified unidentified anomalies as major ones, highlighting the need for further improvement, particularly in refining the determination of threshold values for both velocities and displacements.

The developed model presents valuable implications for bridge managers, as it provides a reliable tool for classifying signals obtained from accelerometers installed on any bridge structure. This enables bridge managers to make informed decisions regarding

necessary maintenance and protective measures, which will eventually minimize the future maintenance costs. Notably, the model is currently undergoing integration into the sensor manufactured by Sisgeo company, representing a significant milestone toward practical implementation in monitoring systems.

Looking ahead, future studies should consider exploring unsupervised ML as they offer the potential to reveal latent patterns, which may help understand unidentified signals by revealing underlying patterns or similarities within the data. Additionally, introducing additional features extracted from the frequency power spectrum, such as signal energy, can be essential for enhancing the model. These features can capture valuable information about the distribution and intensity of the signals, contributing to a more comprehensive and accurate classification. Finally, the created system could be extended to encompass other types of bridge structures that are vulnerable to shocks. This may provide further insights to enhance the overall accuracy and generalizability of the system.

Overall, this study presents a significant contribution to the field of railway bridge monitoring. The proposed approach has the potential to significantly improve the safety and reliability of railway bridges by providing early detection of potential collisions and enabling proactive maintenance interventions. Additionally, the developed approach aids in reducing disk storage and saving energy in embedded systems.

## Acknowledgement

The authors acknowledge the valuable contributions of the AUDACE project partners from SNCF-R for providing access to the instrumented bridges and their expertise in dynamic structural behavior, and SISGEO for the instrumentation and project management.

## Funding Support

This work is sponsored by the AUDACE project which is supported by the French Ministry of Ecological Transition, through the grant program “Ponts connectés” managed by the Center of Studies on Risk, Environment, Mobility, and Urban Planning.

## Ethical Statement

This study does not contain any studies with human or animal subjects performed by any of the authors.

## Conflicts of Interest

The authors declare that they have no conflicts of interest to this work.

## Data Availability Statement

Data available on request from the corresponding author upon reasonable request.

## Author Contribution Statement

**Khaled Hallak:** Conceptualization, Methodology, Software, Validation, Formal analysis, Investigation, Resources, Data curation, Writing – original draft, Writing – review & editing, Visualization. **Adel Abdallah:** Conceptualization, Methodology, Investigation, Resources, Writing – review & editing, Supervision, Project administration, Funding acquisition.

## References

[1] SNCF Réseau. (2021). Heurt sur un pont: Contextualisation, caractérisation et mesure des conséquences par l’enstrumentation. AUDACE 2021.

[2] Vagnoli, M., Remenyte-Prescott, R., & Andrews, J. (2018). Railway bridge structural health monitoring and fault detection: State-of-the-art methods and future challenges. *Structural Health Monitoring*, *17*(4), 971–1007. https://doi.org/10.1177/1475921717721137

[3] Zhang, J., & Feng, C. (2018). *Routledge handbook of transport in Asia*. UK: Taylor & Francis Group.

[4] Devi, G. N., & Vijayalakshmi, M. M. (2021). Smart structural health monitoring in civil engineering: A survey. *Materials Today: Proceedings*, *45*(7), 7143–7146. https://doi.org/10.1016/j.matpr.2021.02.095

[5] Fu, Y., Mechitov, K., Hoang, T., Kim, J. R., Memon, S. A., & Spencer, B. F. (2021). Efficient and high-precision time synchronization for wireless monitoring of civil infrastructure subjected to sudden events. *Structural Control and Health Monitoring*, *28*(1), e2643. https://doi.org/10.1002/stc.2643

[6] Avci, O., Abdeljaber, O., Kiranyaz, S., Hussein, M., Gabbouj, M., & Inman, D. J. (2021). A review of vibration-based damage detection in civil structures: From traditional methods to machine learning and deep learning applications. *Mechanical Systems and Signal Processing*, *147*, 107077. https://doi.org/10.1016/j.ymssp.2020.107077

[7] Basharat, A., Catbas, N., & Shah, M. (2005). A framework for intelligent sensor network with video camera for structural health monitoring of bridges. In *Third IEEE International Conference on Pervasive Computing and Communications Workshops,* 385–389. https://doi.org/10.1109/PERCOMW.2005.6

[8] He, Z., Li, W., Salehi, H., Zhang, H., Zhou, H., & Jiao, P. (2022). Integrated structural health monitoring in bridge engineering. *Automation in Construction*, *136*, 104168. https://doi.org/10.1016/j.autcon.2022.104168

[9] Nassif, A. B., Talib, M. A., Nasir, Q., & Dakalbab, F. M. (2021). Machine learning for anomaly detection: A systematic review. *IEEE Access*, *9*, 78658–78700. https://doi.org/10.1109/ACCESS.2021.3083060

[10] Ghiasi, A., Ng, C. T., & Sheikh, A. H. (2022). Damage detection of in-service steel railway bridges using a fine k-nearest neighbor machine learning classifier. *Structures*, *45*, 1920–1935. https://doi.org/10.1016/j.istruc.2022.10.019

[11] Ghiasi, A., Moghaddam, M. K., Ng, C. T., Sheikh, A. H., & Shi, J. Q. (2022). Damage classification of in-service steel railway bridges using a novel vibration-based convolutional neural network. *Engineering Structures*, *264*, 114474. https://doi.org/10.1016/j.engstruct.2022.114474

[12] Wang, C., Gao, J., Li, H., Lin, C., Beck, J. L., & Huang, Y. (2023). Robust sparse Bayesian learning for broad learning with application to high-speed railway track monitoring. *Structural Health Monitoring*, *22*(2), 1256–1272. https://doi.org/10.1177/14759217221104224

[13] Lee, J., Jeong, S., Lee, J., Sim, S. H., Lee, K. C., & Lee, Y. J. (2022). Sensor data-based probabilistic monitoring of time-history deflections of railway bridges induced by high-speed trains. *Structural Health Monitoring*, *21*(6), 2518–2530. https://doi.org/10.1177/14759217211063424

[14] Chalouhi, E. K., Gonzalez, I., Gentile, C., & Karoumi, R. (2017). Damage detection in railway bridges using machine

learning: Application to a historic structure. *Procedia Engineering*, *199*, 1931–1936. https://doi.org/10.1016/j.proeng.2017.09.287

[15] Abdu, D. M., Wei, G., & Yang, W. (2023). Assessment of railway bridge pier settlement based on train acceleration response using machine learning algorithms. *Structures*, *52*, 598–608. https://doi.org/10.1016/j.istruc.2023.03.167

[16] Akintunde, E., Azam, S. E., & Linzell, D. G. (2023). Singular value decomposition and unsupervised machine learning for virtual strain sensing: Application to an operational railway bridge. *Structures*, *58*, 105417. https://doi.org/10.1016/j.istruc.2023.105417

[17] Sabato, A., Niezrecki, C., & Fortino, G. (2017). Wireless MEMS-based accelerometer sensor boards for structural vibration monitoring: A review. *IEEE Sensors Journal*, *17*(2), 226–235. https://doi.org/10.1109/JSEN.2016.2630008

[18] Peng, H., Long, F., & Ding, C. (2005). Feature selection based on mutual information criteria of max-dependency, max-relevance, and min-redundancy. *IEEE Transactions on Pattern Analysis and Machine Intelligence*, *27*(8), 1226–1238. https://doi.org/10.1109/TPAMI.2005.159

[19] Liu, H., & Setiono, R. (1995). Chi2: Feature selection and discretization of numeric attributes. In *Proceedings of 7th IEEE International Conference on Tools with Artificial Intelligence*, 388–391. https://doi.org/10.1109/TAI.1995.479783

[20] McKight, P. E., & Najab, J. (2010). Kruskal-Wallis test. In I. B. Weiner & W. E. Craighead (Eds.), *The Corsini encyclopedia of psychology* (pp. 1–1). Wiley. https://doi.org/10.1002/9780470479216.corpsy0491

[21] Breiman, L. (1996). Bagging predictors. *Machine Learning*, *24*(2), 123–140. https://doi.org/10.1007/BF00058655

[22] Laaksonen, J., & Oja, E. (1996). Classification with learning k-nearest neighbors. In *Proceedings of International Conference on Neural Networks*, *3*, 1480–1483. https://doi.org/10.1109/ICNN.1996.549118

[23] Erbek, F. S., Özkan, C., & Taberner, M. (2004). Comparison of maximum likelihood classification method with supervised artificial neural network algorithms for land use activities. *International Journal of Remote Sensing*, *25*(9), 1733–1748. https://doi.org/10.1080/0143116031000150077

[24] Burges, C. J. C. (1998). A tutorial on support vector machines for pattern recognition. *Data Mining and Knowledge Discovery*, *2*(2), 121–167. https://doi.org/10.1023/A:1009715923555

**How to Cite:** Hallak, K., & Abdallah, A. (2024). A Supervised Machine Learning Monitoring System for Vehicle-Railway Bridge Collision. *Artificial Intelligence and Applications*, *2*(4), 315–329. https://doi.org/10.47852/bonviewAIA42022662